JOURNAL OF CATALYSIS 95, 482–491 (1985)

# Oxidation of Furan on Well-Characterized Vanadium Oxide Catalysts

KENJI MORI,* AKIRA MIYAMOTO,†,[1] AND YUICHI MURAKAMI†

*Kinu-ura Research Department, JGC Corporation, Sunosaki-cho, Handa, Aichi 475, Japan, and
†Department of Synthetic Chemistry, Faculty of Engineering, Nagoya University,
Furo-cho, Chikusa-ku, Nagoya 464, Japan

Received December 5, 1984; revised March 20, 1985

The activity and selectivity in the oxidation of furan on unsupported and supported $V_2O_5$ catalysts were investigated in connection with the catalyst structure. It was found that the steady-state reaction rate at various concentrations of $O_2$ was proportional to the amount of $V^{5+}{=}O$ species in the catalyst, indicating that the surface V=O plays the active oxygen species for the reaction. The specific activity of surface V=O species, defined by the rate per surface V=O, for unsupported $V_2O_5$ changed greatly with the surface structure of the catalyst: The fusion of $V_2O_5$ markedly decreased the specific activity, while the severe redox treatment of the fused catalyst increased it. This means that the furan oxidation on $V_2O_5$ catalysts is a structure-sensitive reaction. The specific activity of the surface V=O species for the $V_2O_5/TiO_2$ and $V_2O_5/Al_2O_3$ catalysts was smaller than that for the unsupported $V_2O_5$, indicating the retarding effect of the support on the activity. This is in contrast to the known promoting effect of $TiO_2$ support on the activity. The selectivity to maleic anhydride was found to be determined by the number of $V_2O_5$ layers on support for both $V_2O_5/TiO_2$ and $V_2O_5/Al_2O_3$ catalysts. When the number of $V_2O_5$ layers was 1 or 2, the selectivity was low, while it increased markedly with the increase in the number of $V_2O_5$ layers to 5, and attained a constant value above 5 layers. The change in the oxidation state of the catalyst did not affect the selectivity. These behaviors in the activity and selectivity in the furan oxidation were discussed in comparison with those in the benzene oxidation.

## INTRODUCTION

Supported metal oxide catalysts exhibit interesting catalysis depending on the kind of support and on the composition of the catalysts (*1–6*). However, the activity and selectivity on the supported metal oxide catalyst have not been well clarified in terms of the structure of the metal oxide on support. This seems to be due to the lack of a well-established method to determine the structure of supported metal oxide catalysts, especially the number of active sites. As for the supported vanadium oxide catalysts, we have previously established the rectangular pulse technique which allows the determination of the number of surface V=O species (*L*) and the number of $V_2O_5$ layers on support(*N*) (*7, 8*). This technique is based on the following reactions:

$$\mathrm{V{=}O + NO + NH_3 \rightarrow V{-}OH + N_2 + H_2O} \quad (1)$$

$$\mathrm{V{-}OH \xrightarrow{\text{bulk V=O}} V{=}O + \tfrac{1}{2}H_2O} \quad (2)$$

together with the introduction of the NO and $NH_3$ mixture in a rectangular pulse to the preoxidized catalyst and the subsequent detection of the concentration profile of $N_2$ produced by Reaction (1). The separation of the $N_2$ formed on the initial surface V=O species from that formed on the reproduced V=O species leads to a determination of *L*, while detailed analysis of the concentration profile of the $N_2$ formed on the reproduced V=O species leads to a determination of *N*. Furthermore, the structures of $V_2O_5/TiO_2$ and $V_2O_5/Al_2O_3$ catalysts have been determined by using various physicochemical measurements together with the rectangular pulse technique (*9–11*).

By investigating the oxidation of benzene on the well-characterized vanadium oxide catalysts, the activity and selectivity in the

---

[1] Present address: Department of Hydrocarbon Chemistry, Faculty of Engineering, Kyoto University, Sakyo-ku, Kyoto 606, Japan.

0021-9517/85 $3.00

benzene oxidation have been revealed in terms of the structure of $V_2O_5$ on the support (*12*): the activity is determined mainly by the number of surface V=O species, and the specific activity of the surface V=O species is modified by the support. The $TiO_2$ support promotes the activity of the surface V=O species, while the $Al_2O_3$ support slightly reduces it. On the other hand, the selectivity to the partial oxidation product (maleic anhydride) is determined by the number of $V_2O_5$ layers on the support for both $V_2O_5/TiO_2$ and $V_2O_5/Al_2O_3$. For the monolayer $V_2O_5$ catalyst, the selectivity is very low and benzene is preferentially oxidized to CO and $CO_2$. As the number of $V_2O_5$ layers on the support increases to 5, the selectivity increases monotonically and the selective oxidation to maleic anhydride proceeds for catalysts with $V_2O_5$ layers of more than 5. Since the structure–activity/selectivity correlation is expected to change greatly with the kind of reactions (*13–23*), it seems interesting to investigate the correlation for various reactions. The purpose of this study is then to reveal the correlation for the furan oxidation. This reaction was selected because the partial oxidation product (maleic anhydride) of the reaction is the same as that in the benzene oxidation while the structures of reactant molecules are significantly different from each other (*24–26*).

## EXPERIMENTAL

### *Catalysts*

An unsupported $V_2O_5$–U catalyst was prepared by the thermal decomposition of $NH_4VO_3$ in a stream of $O_2$ at 773 K. A $V_2O_5$–F catalyst was prepared by fusing the $V_2O_5$–U catalyst at 1073 K for 18 h in air, followed by gradual cooling to room temperature. A $V_2O_5$–RO catalyst was prepared from the $V_2O_5$–F catalyst by the reduction–oxidation treatment, that is, the reduction in flowing $H_2$ at 673 K for 1 h followed by the reoxidation in flowing $O_2$ (20%) at 673 K for 1 h, and this redox cycle was repeated five times.

$TiO_2$ composed of anatase was prepared by hydrolysis of $Ti(SO_4)_2$ followed by calcination in air at 873 K, while $Al_2O_3$ was commercially available (Sumitomo $\gamma$-$Al_2O_3$). BET surface areas of $TiO_2$ and $Al_2O_3$ were 48 and 230 $m^2\ g^{-1}$, respectively. Vanadium oxides supported on the carriers were prepared by impregnation of the carrier with an oxalic acid solution of $NH_4VO_3$ followed by calcination at 773 K in a stream of $O_2$ for 3 h. $V_2O_5/TiO_2$ and $V_2O_5/Al_2O_3$ monolayer catalysts were prepared by treating $V_2O_5/TiO_2$ (10 mol% $V_2O_5$) and $V_2O_5/Al_2O_3$ (25 mol% $V_2O_5$), respectively, with 0.3 *N* $NH_4OH$ solution for 48 h, followed by drying, and subsequent calcination at 773 K in a stream of $O_2$ for 3 h (*27*). Unless otherwise stated, particle size of the catalyst ranged from 28 to 48 mesh.

### *Characterizations of Catalysts*

The number of surface V=O species (*L*) on the catalyst was determined by using the rectangular pulse technique (*7, 8*) under the following conditions: flow rate of the car-

TABLE 1

Physical and Catalytic Properties of Unsupported $V_2O_5$ Catalysts[a,b]

| Catalyst | $S_{BET}$ ($m^2\ g^{-1}$) | $L$ ($\mu mol\ g^{-1}$) | $L/S_{BET}$ ($\mu mol\ m^{-2}$) | $R$ ($\mu mol\ g^{-1}\ s^{-1}$) | $R/S_{BET}$ ($\mu mol\ m^{-2}\ s^{-1}$) | TF ($k\ s^{-1}$) | S(MA) (%) | $S(CO + CO_2)$ (%) | $S(CO)/S(CO_2)$ |
|---|---|---|---|---|---|---|---|---|---|
| $V_2O_5$–U | 5.4 | 22 | 4.1 | 9.98 | 1.84 | 454 | 77 | 23 | 0.54 |
| $V_2O_5$–F | 0.8 | 4 | 5.0 | 0.51 | 0.64 | 128 | 75 | 25 | 0.52 |
| $V_2O_5$–RO | 0.8 | 4 | 5.0 | 0.77 | 0.96 | 193 | 76 | 24 | 0.56 |

[a] $S_{BET}$, the BET (Brunauer–Emmett–Teller) surface area; *L*, the number of surface V=O species; *R*, reaction rate; S(MA), selectivity to maleic anhydride; $S(CO + CO_2)$, selectivity to CO and $CO_2$; S(CO), selectivity to CO; $S(CO_2)$, selectivity to $CO_2$.

[b] Reaction conditions: temperature 622 K; $P_F = 0.0074$ atm; $P_O = 0.397$ atm.

rier gas(He) = 150 $cm^3$ $min^{-1}$; concentration of NO = $4.86 \times 10^{-8}$ mol $cm^{-3}$; concentration of $NH_3$ = $9.25 \times 10^{-7}$ mol $cm^{-3}$; pulse width = 60 s; temperature = 520–630 K. Results of $L$ for the unsupported $V_2O_5$ are shown in Table 1 together with the results of the BET surface area ($S_{BET}$). The number of $V_2O_5$ layers ($N$) for the catalysts was calculated from $L$ by

$$N = 2/[LM(V_2O_5)], \tag{3}$$

where $M(V_2O_5)$ is molecular weight of $V_2O_5$. According to the results of X-ray diffraction, UV–visible spectra, IR spectra, X-ray photoelectron spectra, and scanning electron micrographs (*13, 14*), electronic properties of the catalysts do not change from each other while the surface of $V_2O_5$–U or $V_2O_5$–RO is rougher than that of $V_2O_5$–F.

The $L$, $N$, and $S_{BET}$ of the supported catalysts have similarly been determined (*8–11*) and the results are shown in Table 2. $ML$ is the percentage theoretical monolayer of $V_2O_5$ (*28*), which is calculated from the $V_2O_5$ content ($x$) and $S_{BET}$ by

$$ML = \frac{N_A x \sigma(V_2O_5)}{xM(V_2O_5) + (1 - x)M(\text{support})} \frac{100}{S_{BET}} (\%), \tag{4}$$

where $N_A$ is the Avogadro number; $\sigma(V_2O_5)$ is the area occupied by a $V_2O_5$ unit(20.6 Å$^2$); and $M$(support) is molecular weight of support ($TiO_2$ or $Al_2O_3$).

A catalyst in the steady-state reaction was rapidly cooled down to a room temperature under the inert-gas condition ($N_2$ or He) to measure the steady-state catalyst structure. IR spectra of the catalyst were observed on a Jasco-EDR-31 emissionless IR diffuse reflectance spectrometer using KBr as a diluent (*29*).

### *Catalytic Activity Measurements*

Kinetic studies were carried out by using the continuous flow reaction technique under the following conditions; total pressure = 1 atm (1 atm = 101.3 kPa), temperature = 583–653 K, partial pressure of $O_2$ ($P_O$) = 0–0.397 atm, partial pressure of furan ($P_F$) = 0.0074 atm, $W/F$ = 60.2–7510 g s $mol^{-1}$, and nitrogen was used as a balance gas.

TABLE 2

Physical and Catalytic Properties of $V_2O_5/TiO_2$ and $V_2O_5/Al_2O_3$ Catalysts[a,b]

| Catalyst (mol% $V_2O_5$) | $S_{BET}$ ($m^2$ $g^{-1}$) | $L$ (μmol $g^{-1}$) | $N$ | ML (%) | $R$ (μmol $g^{-1}$ $s^{-1}$) | TF ($k$ $s^{-1}$) | $S$(MA) (%) | $S(CO + CO_2)$ (%) | $S(CO)/S(CO_2)$ |
|---|---|---|---|---|---|---|---|---|---|
| $V_2O_5/TiO_2$ | | | | | | | | | |
| 1 | 47 | 56 | 1–2 | 32 | 4.57 | 82 | 43 | 57 | 0.21 |
| 2 | 45 | 120 | 1–2 | 67 | 8.50 | 71 | 49 | 51 | 0.22 |
| 5 | 26 | 184 | 2–3 | 280 | 35.0 | 190 | 73 | 27 | 0.36 |
| 10 | 23 | 135 | 5–8 | 600 | 35.9 | 266 | 79 | 21 | 0.60 |
| 25 | 10 | 60 | 30–40 | 2800 | 25.3 | 422 | 78 | 22 | 0.65 |
| 50 | 7.4 | 31 | 50–60 | 6400 | 14.8 | 477 | 79 | 21 | 0.53 |
| Monolayer | 32 | 126 | 1 | – | 13.6 | 108 | 46 | 54 | 0.41 |
| $V_2O_5/Al_2O_3$ | | | | | | | | | |
| 2 | 221 | 3 | 1–2 | 11 | 0.48 | 160 | 12 | 88 | 0.12 |
| 5 | 219 | 77 | 1–2 | 27 | 7.55 | 98 | 40 | 60 | 0.43 |
| 10 | 168 | 355 | 1–3 | 67 | 29.0 | 82 | 64 | 36 | 0.45 |
| 25 | 114 | 405 | 2–4 | 220 | 40.5 | 100 | 64 | 36 | 0.62 |
| 35 | 101 | 365 | 3–7 | 330 | 25.8 | 71 | 72 | 28 | 0.61 |
| 50 | 66 | 249 | 5–15 | 660 | 26.3 | 106 | 70 | 30 | 0.56 |
| Monolayer | 174 | 20 | 1 | – | 2.21 | 110 | 32 | 68 | 0.37 |
| $V_2O_5$–U | 5.4 | 22 | 504 | | 9.98 | 454 | 77 | 23 | 0.54 |

[a] $N$, number of $V_2O_5$ layers on support; ML, percentage theoretical monolayer of $V_2O_5$ calculated by Eq. (2); see Table 1 for the definitions of $S_{BET}$, $L$, $R$, TF, $S$(MA), $S(CO + CO_2)$, $S$(CO), and $S(CO_2)$.

[b] Reaction conditions: temperature, 622 K; $P_F$ = 0.0074 atm; $P_O$ = 0.397 atm.

Maleic anhydride (MA), CO, and $CO_2$ were identified as reaction products. Rate of formation of MA was determined by titration with 0.1 *N* NaOH after its collection with water. CO and $CO_2$ were analyzed by using gas chromatography. Particular care was taken in eliminating the heat of reaction, and therefore controlling the reactor temperature ($\pm 1$ K). The glass reactor was heated to the reaction temperature by using a fluidized bed of sand, and the catalyst was diluted with $\alpha$-$Al_2O_3$.

## RESULTS

### *Effects Of $O_2$ Partial Pressure on Reaction Rates and Catalyst Structures*

In the oxidation of furan on vanadium oxide catalysts, the following reactions were found to take place:

$$C_4H_4O(FR) \xrightarrow{O_2} C_4H_2O_3(MA) \quad (5)$$

$$C_4H_4O(FR) \xrightarrow{O_2} 4CO \quad (6)$$

$$C_4H_4O(FR) \xrightarrow{O_2} 4CO_2. \quad (7)$$

From the stoichiometries of Eqs. (3)–(5), the rate of formation of each product [$R$(MA), $R$(CO), or $R(CO_2)$] is defined as the rate of furan converted to the product. The rate of formation of the total oxidation products(CO and $CO_2$)[$R(CO + CO_2)$] is defined by

$$R(CO + CO_2) = R(CO) + R(CO_2). \quad (8)$$

The total reaction rate($R$) and selectivities to partial oxidation product [$S(MA_2)$], total oxidation products [$S(CO + CO_2)$], CO[$S$(CO)], and $CO_2$[$S(CO_2)$] are, respectively,

$$R = R(MA) + R(CO + CO_2) \quad (9)$$

$$S(MA) = R(MA)/R \quad (10)$$

$$S(CO + CO_2) = R(CO + CO_2)/R \quad (11)$$

$$S(CO) = R(CO)/R \quad (12)$$

$$S(CO_2) = R(CO_2)/R. \quad (13)$$

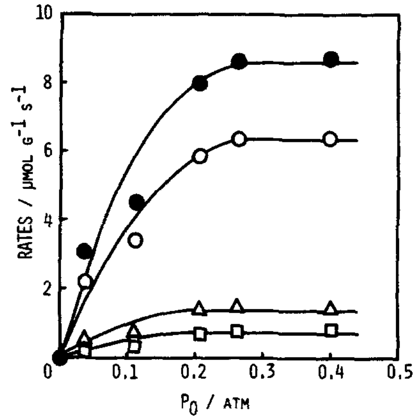

FIG. 1. Effect of $P_O$ on $R$, $R$(MA), $R$(CO), and $R(CO_2)$ for the $V_2O_5$–U at 615 K: (●) $R$; (○) $R$(MA); (□) $R$(CO); (△) $R(CO_2)$; $P_F$ = 0.0074 atm; $W/F$ = 164.1 g s mol$^{-1}$.

Figure 1 shows effects of $P_O$ on $R$, $R$(MA), $R$(CO), and $R(CO_2)$ for the $V_2O_5$–U catalyst at 615 K. The rates increased gradually with increasing $P_O$ to 0.262 atm, while they were almost constant at $P_O$ above 0.262 atm. In spite of the change of the reaction rates with $P_O$, $S$(MA), $S$(CO), and $S(CO_2)$ were independent of $P_O$ as shown in Fig. 2.

According to the results of change in the reaction rates after the stoppage of the $O_2$ gas supply, the rates decreased gradually with increasing time and attained a negligible value at 8 h after the reaction began. It was also confirmed that both the reaction

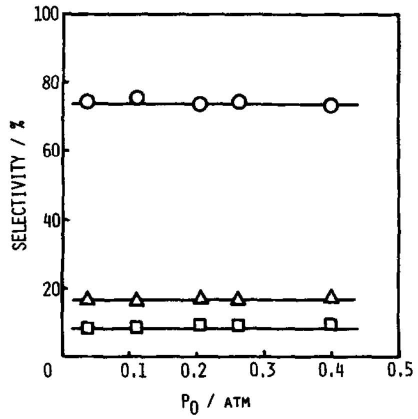

FIG. 2. Effect of $P_O$ on $S$(MA), $S$(CO), and $S(CO_2)$ for the $V_2O_5$–U at 615 K: (○) $S$(MA); (□) $S$(CO); (△) $S(CO_2)$; $P_F$ = 0.0074 atm.

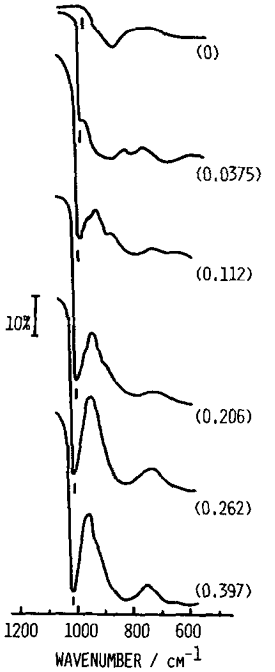

Fig. 3. Infrared spectra of the $V_2O_5$–U in the steady state of furan oxidation at various partial pressures of $O_2$. Reaction temperature = 615 K, $P_F$ = 0.0074 atm. The number in parentheses represents the partial pressure of $O_2$.

rate and infrared spectrum of the catalyst attained a steady state under this condition. Figure 3 shows IR spectra of the $V_2O_5$–U catalyst in the steady-state reaction at various partial pressures of $O_2$. The catalyst in the steady-state reaction above 0.262 atm of $P_O$ gave absorption bands at 1020 and 825 cm$^{-1}$ which are assigned to the stretching vibration of V=O species and the coupled vibration between V=O and V—O—V species, respectively (*30, 31*). The absorption at 1020 and 825 cm$^{-1}$ gradually decreased as $P_O$ decreased below 0.262 atm, and new absorption bands at 990 and 910 cm$^{-1}$ were observed for the catalyst in the steady-state reaction below 0.112 atm of $P_O$. These bands are assigned to lattice vibrations of $V_2O_4$ (*32*). In order to quantitate the change in the amount of V=O species with $P_O$, relative absorbance at 1020 cm$^{-1}$ was calculated from the spectra in Fig. 3, and the results are shown in Fig. 4. As shown, the amount of V=O species increases almost linearly with $P_O$ to 0.262 atm, and it is constant above this value of $P_O$.

### *Activity and Selectivity in Furan Oxidation under Excess Oxygen Conditions*

Table 1 shows results of $R$, $R/S_{BET}$, $S$(MA), $S(CO + CO_2)$, and $S(CO)/S(CO_2)$ for unsupported vanadium oxide catalysts under excess oxygen conditions where the reaction rate was zeroth order with respect to $P_O$ and where the catalyst was confirmed to be in the highest oxidation state, i.e., $V^{5+}$. In accordance with the decrease in $S_{BET}$, $R$ for $V_2O_5$–F or $V_2O_5$–RO was much smaller than that for $V_2O_5$–U. It should be noted that the $R/S_{BET}$ for $V_2O_5$–U is much larger than that for $V_2O_5$–F, and the $R/S_{BET}$ for $V_2O_5$–RO is larger than that for $V_2O_5$–F. In contrast to the behavior in the reaction rate, the selectivity, $S$(MA), $S(CO + CO_2)$, or $S(CO)/S(CO_2)$, did not change significantly with the kind of unsupported $V_2O_5$.

Table 2 shows results of $R$, $S$(MA), $S(CO + CO_2)$, and $S(CO)/S(CO_2)$ for $V_2O_5/TiO_2$ and $V_2O_5/Al_2O_3$ catalysts with various $V_2O_5$ contents. $TiO_2$ or $Al_2O_3$ alone had a negligible activity for the furan oxidation. The reaction rate ($R$) for $V_2O_5/TiO_2$ increased

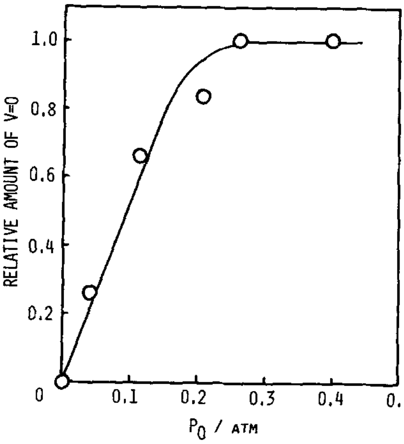

Fig. 4. Amount of V=O in the $V_2O_5$–U in the steady state of furan oxidation at various partial pressures of $O_2$.

markedly with an increase in $V_2O_5$ content from 0 to 10 mol%, passed a maximum at 10 mol% $V_2O_5$, and then decreased to the value of $V_2O_5$–U with further increase in $V_2O_5$ content. The selectivity to MA[$S$ (MA)] was low for $V_2O_5/TiO_2$ containing 1 or 2 mol% $V_2O_5$, while it reached as high as 70% for catalysts with $V_2O_5$ content above 5 mol%. $V_2O_5/Al_2O_3$ with low $V_2O_5$ content (2 mol%) had only a negligible activity. $R$ increased markedly with increasing $V_2O_5$ content from 5 to 25 mol%. $R$ for $V_2O_5/Al_2O_3$ (25 mol% $V_2O_5$) was considerably higher than $R$ for $V_2O_5/TiO_2$ (5 mol% $V_2O_5$). $S$(MA) for $V_2O_5/Al_2O_3$ with low $V_2O_5$ content (2 or 5 mol%) was very low, while it increased markedly in the range from 5 to 25 mol% and attained a constant value above 25 mol%. $S$(MA) for the monolayer $V_2O_5/TiO_2$ and $V_2O_5/Al_2O_3$ was low, and total oxidation of furan to CO and $CO_2$ takes place preferentially. Although Tables 1 and 2 show results for the reaction at 622 K, similar relationships were found to hold at any temperature examined (583–653 K): Apparent activation energy for $R$ was 20–22 kcal/mol for the unsupported $V_2O_5$ catalysts, 20–21 kcal/mol for $V_2O_5/TiO_2$, and 22–23 kcal/mol for $V_2O_5/Al_2O_3$.

## DISCUSSION

### *Active Oxygen Species for the Furan Oxidation*

As shown in Fig. 1, the rate of furan oxidation increased with increasing $P_O$ to 0.262 atm for $V_2O_5$–U and attained a constant value above this value of $P_O$. The steady-state amount of the $V^{5+}{=}O$ species in the catalyst changed with $P_O$ similarly to the reaction rate (Fig. 4). This suggests that the reaction proceeds by the reduction–oxidation mechanism (or Mars–van Krevelen mechanism) (*33*) and that the active oxygen species for the furan oxidation is surface V=O species. The IR band at 1020 $cm^{-1}$ is usually monitoring the change in the concentration of the bulk V=O, and not that of the surface V=O species. Under the steady-state reaction conditions, however, the band is expected to show the concentration of the surface V=O species, since the surface is in equilibrium with the bulk under the conditions. Adsorbed oxygen species are not responsible for this reaction, because no adsorbed oxygen species, such as $O_2^-$, $O^-$, or $O_3^-$, were detected on the catalysts by either ESR or TPD measurement. The observed relationship between reaction rate and $P_O$ (Fig. 1) can be explained in terms of the reduction–oxidation mechanism as follows: In the absence of $O_2$ ($P_O$ = 0 atm), the catalyst is in the reduced state and no surface V=O species is present to oxidize furan. As $P_O$ increases, the reoxidation of the reduced catalyst by $O_2$ increase the oxidation state of the catalyst to increase the number of surface V=O species. This means that the reaction rate increases with increasing $P_O$. In the presence of excess oxygen ($P_O > 0.262$ atm), the catalyst is in the highest oxidation state, i.e., $V_2O_5$. Therefore, the increase in $P_O$ does not lead to further increase in the oxidation state or the number of surface V=O species, and the reaction rate does not increase with $P_O$ under excess oxygen conditions.

### *Structure Sensitivity of the Reaction*

The surface of $V_2O_5$–F has been found to be significantly different from that of $V_2O_5$–U or $V_2O_5$–RO (*13, 14*). Since the surface V=O species has been found to be the active oxygen species for the furan oxidation, turnover frequency (TF) for this reaction can be defined by

$$TF = R/L. \qquad (14)$$

Values of TF at 622 K were calculated from the results of $R$ and $L$ (Table 1) for various catalysts, and the results are also shown in Table 1. It is evident from Table 1 that TF changes significantly with the kind of catalysts; TF for $V_2O_5$–U is much larger than TF for $V_2O_5$–F, and TF for $V_2O_5$–RO is larger than TF for $V_2O_5$–F. These behaviors in the furan oxidation are in contrast to those in the benzene oxidation (*12*) and indicate that the furan oxidation on $V_2O_5$ catalysts is a structure-sensitive reaction. Fusion of a solid would generally lead to a smooth surface with a decreased number of surface defects (e.g., steps, kinks, or vacancies), while severe redox treatment of a solid with few surface defects would tend to increase their number. Furthermore, no impurity peaks were observed in the XPS spectrum of the $V_2O_5$–U, $V_2O_5$–F, or $V_2O_5$–RO. Since the surface V=O species has been shown to be the active oxygen species, the surface V=O species at the surface defects are considered to be much more active than that in the smooth (010) plane.

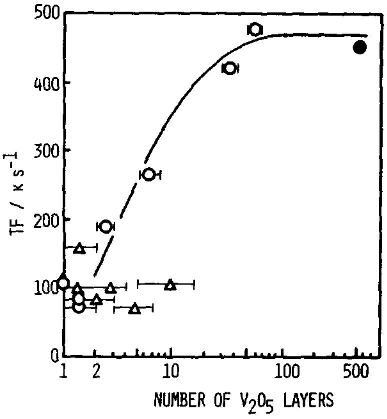

FIG. 5. Relationship between the turnover frequency (TF) for furan oxidation and the number of $V_2O_5$ layers on support: (○) $V_2O_5/TiO_2$; (△) $V_2O_5/Al_2O_3$; (●) $V_2O_5$–U.

*Activity of Supported Catalysts*

In general, the activity of supported catalysts is determined by two factors: (i) the number of active sites and (ii) the specific activity of the active site, that is, the turnover frequency. The separation of these two factors is indispensable for detailed understanding the role of the support in a given reaction. As shown in Table 2, the rate (*R*) for $V_2O_5/Al_2O_3$ and $V_2O_5/TiO_2$ catalysts is larger than that for $V_2O_5$–U, indicating the promoting effect of the $Al_2O_3$ or $TiO_2$ support. The number of surface V=O species (*L*) for $V_2O_5/Al_2O_3$ and $V_2O_5/TiO_2$ catalysts is much larger than that for the unsupported $V_2O_5$, while the turnover frequency (TF) for the supported catalysts is smaller than that for the $V_2O_5$–U. This means that the promoting effect of $Al_2O_3$ or $TiO_2$ is to increase the number of surface V=O species, but the specific activity of the surface V=O species is not increased by the support. Figure 5 shows the relationship between the turnover frequency (TF) and the number of $V_2O_5$ layers (*N*) for $V_2O_5/TiO_2$ and $V_2O_5/Al_2O_3$. The turnover frequency for $V_2O_5/TiO_2$ decreases monotonically with decreasing the number of $V_2O_5$ layers on $TiO_2$. This indicates that the retarding effect of $TiO_2$ on the specific activity of the surface V=O species becomes greater with the decreasing number of $V_2O_5$ layers.

According to Vejux and Courtine (*34*), there is remarkable fit of the crystallographic patterns between the (010) face of $V_2O_5$ and the $TiO_2$ surface. It is therefore considered that a smooth $V_2O_5$ surface with few defects is formed for the $V_2O_5/TiO_2$ catalysts having a low concentration of $V_2O_5$, and that the number of surface defects increases with increasing content of $V_2O_5$. Since the activity of the surface V=O species at the surface defect is much higher than that in the smooth (010) face, this explains the significant reduction in the turnover frequency for $V_2O_5/TiO_2$ compared with that for $V_2O_5$–U and the increase of the turnover frequency with increasing content of $V_2O_5$ in $V_2O_5/TiO_2$

For both furan oxidation and benzene oxidation, the surface V=O species plays the active oxygen species and maleic anhydride is formed as a partial oxidation product. However, the structural requirement of the active site for furan oxidation is significantly different from that for benzene oxidation: The roughness of the catalyst surface greatly affects the activity for furan oxidation, while it does not affect the activity for benzene oxidation (*12*). In other words, the surface V=O species at the surface defects is considered to be much more active than that in smooth (010) face of $V_2O_5$ for furan oxidation, while the specific activity of the surface V=O species for benzene oxidation is not changed by the roughness of the catalyst surface. In accordance with the difference in the structural requirement of the active site, the activity of the $V_2O_5/TiO_2$ catalyst changes greatly with the kinds of reactions. The specific activity of the surface V=O species is increased by supporting $V_2O_5$ on $TiO_2$ for benzene oxidation (*12*), while it is decreased for furan oxidation (Fig. 5). Benzene is a nonpolar cyclic planar molecule, whereas furan is a polar cyclic molecule having an oxygen atom. Such a difference in the structure and property of reactant molecule may be responsible for the difference in the structural requirement of the active site. Further discussion about the reason for the difference will be made in a subsequent paper on the basis of additional data including those of $^{18}O$-tracer experiments.

### *Selectivity in Furan Oxidation*

Figure 6 shows relationships between the selectivity to partial oxidation product [*S*(MA)] and the conversion of furan, which were obtained from the results under excess oxygen conditions at various temperatures. As shown, *S*(MA) is independent of the conversion for any catalyst. This indicates that consecutive oxidation of the partial oxidation product to CO or $CO_2$ was negligible under the present experimental conditions. In other words, the difference in the selectivity among catalysts is not brought about by the consecutive oxidation of the partial oxidation product.

As shown in Fig. 4, the oxidation state of the $V_2O_5$–U catalyst changes greatly with $P_O$. Under the excess oxygen condition, the catalyst is kept in the highest oxidation state, i.e., $V^{5+}$, while it is reduced as $P_O$ decreases. As shown in Fig. 2, *S*(MA), *S*($CO_2$), and *S*(CO) do not change with $P_O$. This means that the selectivity in furan oxidation is independent of the oxidation state of the catalyst at least under the present experimental conditions where conversion of furan is below 40% and consecutive oxidation of the partial oxidation product to CO and $CO_2$ is negligible, and where the catalyst is in its steady state at a given level of $P_O$.

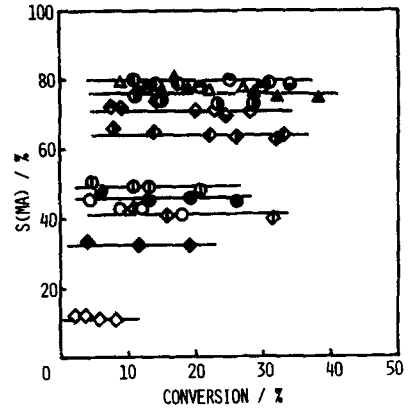

FIG. 6. Relationship between the conversion and selectivity for furan oxidation on unsupported $V_2O_5$, $V_2O_5/TiO_2$, and $V_2O_5/Al_2O_3$ catalysts: (△) $V_2O_5$–U; (▲) $V_2O_5$–F; (▲) $V_2O_5$–RO; (○,⦶,◑,◐,◓,◒,●) $V_2O_5/TiO_2$ with $V_2O_5$ contents, 1, 2, 5, 10, 25, 50, and the monolayer catalyst, respectively. (◇,⟐,⬗,⬖,⬘,⬙,◆) $V_2O_5/Al_2O_3$ with $V_2O_5$ contents 2, 5, 10, 25, 35, 50, and the monolayer catalyst, respectively. Reaction temperature = 583–653 K, $P_F$ = 0.0074 atm, $P_O$ = 0.397 atm.

As shown in Table 1, the selectivity is almost independent of the kind of unsupported $V_2O_5$ catalysts, in contrast to the behavior in the activity of the catalyst. This indicates that the selectivity is not affected by the change in the surface roughness. As shown in Table 2, the selectivity under the excess $O_2$ condition changes greatly with the catalysts. Figure 7 shows results of the selectivity to partial oxidation products [*S*(MA)] against the number of $V_2O_5$ layers on support(*N*). When *N* is 1 or 2, *S*(MA) is low, while it increases markedly with the increase in *N* to 5, and attains a constant value above 5 layers. It is interesting to note that the relationship between *S*(MA) and *N* is almost common to both $V_2O_5/TiO_2$ and $V_2O_5/Al_2O_3$ catalysts, while

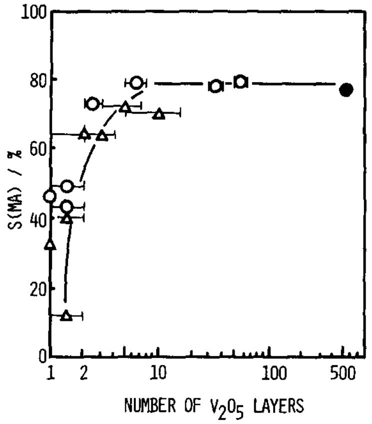

FIG. 7. Relationship between the selectivity and the number of $V_2O_5$ layers on support: (○) $V_2O_5/TiO_2$; (△) $V_2O_5/Al_2O_3$; (●) $V_2O_5$–U.

the structures of the $V_2O_5/TiO_2$ catalysts differ significantly from those of $V_2O_5/Al_2O_3$ catalysts (*9–11*). This indicates that the number of $V_2O_5$ layers is an important factor for determining the selectivities in the oxidation of furan; $V_2O_5$ layers are necessary for the selective oxidation of furan to MA.

The structure–selectivity correlation for furan oxidation is similar to that for benzene oxidation(*12*). The roughness of the catalyst surface does not affect the selectivity for both reactions. The number of $V_2O_5$ layers is an important factor for determining the selectivity for both reactions: the monolayer catalyst exhibits low selectivity to the partial oxidation product, and $V_2O_5$ layers are necessary for the selective oxidation. Although further studies are necessary to clarify molecular mechanism for the correlation between $S$(MA) and $N$, a discussion similar to that described for the benzene oxidation may be applicable to the furan oxidation: As described above, the reaction proceeds by the reduction–oxidation mechanism, and the surface V=O species plays the active oxygen species. It has also been shown that there exists a Brønsted acid site adjacent to the surface V=O species on the supported vanadium oxide catalyst (*9–11, 30*). These suggest that the furan molecule is adsorbed and activated on the Brønsted acid site and that the reaction is initiated by the nucleophilic attack of the oxygen atom of surface V=O species to the adsorbed furan molecule to form an intermediate species. Judging from the stoichiometry of the reaction [Eq. (3)], subsequent introduction of oxygen atoms to the intermediate species is necessary to complete the reaction. Since the reaction proceeds by the reduction–oxidation mechanism, these oxygen atoms are not directly supplied from gaseous $O_2$ but supplied through the oxygen of the catalyst. It is well known that the oxygen of $V_2O_5$ can migrate from the bulk to the surface. When the $V_2O_5$ layers on support are thick enough, the oxygen in the $V_2O_5$ layers can therefore be supplied to oxidize the intermediate species. As for a catalyst with monolayer $V_2O_5$ or with very thin $V_2O_5$ layers on the support, the oxygen cannot be supplied from the bulk, but is supplied by the migration of surface oxygen. This change is the mode of oxidation of the intermediate species with the number of $V_2O_5$ layers ($N$) may provide one of the reasons for the correlation between $S$(MA) and $N$. The change in $S(CO)/S(CO_2)$ with the catalysts (Table 2) may also be explained by the change in the mode of oxidation of the intermediate species.

## ACKNOWLEDGMENTS

This work was partially supported by a grant-in-aid for Scientific Research (59470097) and for Encouragement of Young Scientists (59750655) from the Ministry of Education, Science, and Culture, Japan.

## REFERENCES

1. Hucknall, D. J., "Selective Oxidation of Hydrocarbons." Academic Press, New York, 1974.
2. Wainwright, M. S., and Foster, N. R., *Catal. Rev.* **19,** 211 (1979).
3. Dadyburjor, D. B., Jewur, S. S., and Ruckenstein, E., *Catal. Rev.* **19,** 293 (1979).
4. Bielański, A., and Haber, J., *Catal. Rev.* **19,** 1 (1979).
5. Cullis, C. F., and Hucknall, D. J., "Catalysis," Vol. 5, p. 273. The Chemical Society, London, 1982.
6. Haber, J., *in* "Proceedings, 8th International Congress Catalysis, West Berlin," I-85 (1984).

7. Miyamoto, A., Yamazaki, Y., Inomata, M., and Murakami, Y., *J. Phys. Chem.* **85**, 2366 (1981).
8. Inomata, M., Miyamoto, A., and Murakami, Y., *J. Phys. Chem.* **85**, 2372 (1981).
9. Inomata, M., Mori, K., Miyamoto, A., Ui, T., and Murakami, Y., *J. Phys. Chem.* **87**, 754 (1983).
10. Inomata, M., Mori, K., Miyamoto, A., and Murakami, Y., *J. Phys. Chem.* **87**, 761 (1983).
11. Murakami, Y., Inomata, M., Mori, K., Ui, T., Suzuki, K., Miyamoto, A., and Hattori, T., *in* "Preparation of Catalysts III" (G. Poncelet, P. Grange, and P. A. Jacobs, Eds.), p. 531. Elsevier, Amsterdam, 1983.
12. Mori, K., Inomata, M., Miyamoto, A., and Murakami, Y., *J. Chem. Soc. Faraday Trans. 1* **80**, 2655 (1984).
13. Mori, K., Miyamoto, A., and Murakami, Y., *J. Phys. Chem.* **88**, 2735 (1984).
14. Mori, K., Miyamoto, A., and Murakami, Y., *J. Phys. Chem.* **88**, 2741 (1984).
15. Mori, K., Miura, M., Miyamoto, A., and Murakami, Y., *J. Phys. Chem.* **88**, 5232 (1984).
16. Miyamoto, A., Mori, K., Inomata, M., and Murakami, Y., *in* "Proceedings, 8th International Congress Catalysis, West Berlin," IV-285 (1984).
17. Bond, G. C., and Brückman, K., *Faraday Discuss. Chem. Soc.* **72**, 235 (1981).
18. Cole, D. J., Cullis, C. F., and Hucknall, D. J., *J. Chem. Soc. Faraday Trans. 1* **72**, 2185 (1976).
19. Srivastava, R. D., and Stiles, A. B., *J. Catal.* **77**, 192 (1982).
20. van Hengstum, A. J., van Ommen, J. G., Bosch, H., and Gellings, P. J., *in* "Proceedings, 8th International Congress on Catalysis, West Berlin," IV-297 (1984).
21. Koziolowski, R., Pettifier, R. F., and Thomas, J. M., *J. Phys. Chem.* **87**, 5175 (1983).
22. Ono, T., Nakagawa, Y., Miyata, H., and Kubokawa, Y., *Bull. Chem. Soc. Jpn.* **57**, 1205 (1984).
23. Wachs, I. E., Chan, S. S., Chersich, C. C., and Saleh, Y., *in* "Catalysis on the Energy Scene" (S. Kaliaguine and A. Mahay, Eds.), p. 275. Elsevier, Amsterdam, 1984.
24. Ai, M., *Bull. Chem. Soc. Jpn.* **43**, 3490 (1970).
25. Akimoto, M., and Echigoya, E., *J. Chem. Soc. Faraday Trans. 1* **73**, 193 (1977).
26. Ai, M., Harada, K., and Suzuki, K., *Kogyo Kagaku Zasshi* **73**, 524 (1970).
27. Yoshida, S., Iguchi, T., Ishida, S., and Tarama, K., *Bull. Chem. Soc. Jpn.* **45**, 476 (1972).
28. Roozeboom, F., Fransen, T., Mars, P., and Gellings, P. J., *Z. Anorg. Allg. Chem.* **25**, 449 (1979).
29. Niwa, M., Hattori, T., Takahashi, M., Shirai, K., Watanabe, M., and Murakami, Y., *Anal. Chem.* **51**, 46 (1979).
30. Inomata, M., Miyamoto, A., and Murakami, Y., *J. Catal.* **62**, 140 (1980).
31. Tarama, K., Yoshida, S., Ishida, S., and Kakioka, H., *Bull. Chem. Soc. Jpn.* **41**, 2840 (1969).
32. Frederickson, L. D., and Hansen, D. M., *Anal. Chem.* **35**, 818 (1963).
33. Mars, P., and van Krevelen, D. W., *Chem. Eng. Sci.* **3**, 41 (1951).
34. Vejux, A., and Courtine, P., *J. Solid State Chem.* **23**, 93 (1978).